THE JOURNAL OF PHYSICAL CHEMISTRY B

ARTICLE

pubs.acs.org/JPCB

Reaction Kinetics and Mechanism of Magnetic Field Effects in Cryptochrome

Ilia A. Solov'yov*,† and Klaus Schulten*,†,‡

†Beckman Institute for Advanced Science and Technology, University of Illinois at Urbana−Champaign, Champaign, Illinois 61820, United States

‡Department of Physics, University of Illinois at Urbana−Champaign, Champaign, Illinois 61820, United States

Supporting Information

ABSTRACT: Creatures as varied as mammals, fish, insects, reptiles, and birds have an intriguing sixth sense that allows them to orient themselves in the Earth's magnetic field. Despite decades of study, the physical basis of this magnetic sense remains elusive. A likely mechanism is furnished by magnetically sensitive radical pair reactions occurring in the retina, the light-sensitive part of animal eyes. A photoreceptor, cryptochrome, has been suggested to endow birds with magnetoreceptive abilities as the protein has been shown to exhibit the biophysical properties required for an animal magnetoreceptor to operate properly. Here, we propose a theoretical analysis method for identifying cryptochrome's signaling reactions involving comparison of measured and calculated reaction kinetics in cryptochrome. Application of the method yields an exemplary light-driven reaction cycle, supported through transient absorption and electron-spin-resonance observations together with known facts on avian magnetoreception. The reaction cycle permits one to predict magnetic field effects on cryptochrome activation and deactivation. The suggested analysis method gives insight into structural and dynamic design features required for optimal detection of the geomagnetic field by cryptochrome and suggests further experimental and theoretical studies.

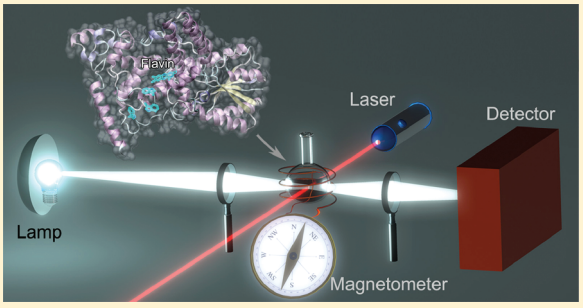

INTRODUCTION

Migratory birds travel annually thousands of kilometers, navigating by using various cues, including the Earth's magnetic field;[1−5] nonmigrant bird species utilize the geomagnetic field similarly to find their way back to the breeding nest;[6−10] but how do birds detect the geomagnetic field? This question focuses on one of the most fascinating unsolved mysteries of sensory biology. At a first glance, tiny iron-oxide particles detected in the upper beak of some bird species[11−16] provide a natural explanation for the avian magnetic compass sense, but behavioral studies revealed that the ability of night-migrating birds to perform magnetic compass orientation is affected by the ambient light,[17−21] which does not penetrate through the beak skin. The latter observation lead to the suggestion that a photochemical reaction in the bird's eyes produces spin-correlated radical pairs that act as the sensor embodying a magnetic field-dependent signaling cascade.[22−27] This suggestion is based on the observation that the recombination reactions of spin-correlated radical pairs can be magnetic field-sensitive.[28,29] The radical pair hypothesis gained stronger support when it was experimentally demonstrated that the magnetic compass in birds is still functioning properly after the iron-mineral-based receptors in the beak are deactivated.[30−33]

Spin-correlated radical pairs are typically created in a photochemical reaction that produces radicals from a molecular precursor in either an electronic singlet (S) or triplet (T) state. Under the influence of intramolecular electron−nuclear hyperfine interactions, the radical pair oscillates between the S and T states, a process known as S ↔ T interconversion. External static magnetic fields affect the rate of this process and, hence, alter the yields of the respective reaction products formed from the S and T radical pairs.[29,34−39] During the last years, the radical-pair hypothesis of the avian magnetic compass gained significant experimental[40−44] and theoretical[22−27,45,46] support. The first experimental proof-of-principle, demonstrating that under a static magnetic field, as weak as that of the Earth, a chemical reaction can act as a magnetic compass by producing detectable changes in the chemical product yield, was achieved for a carotenoid-porphyrin-fullerene model system.[47]

However, for the radical-pair mechanism to play a role in magnetoreception, molecules with certain biophysical characteristics must exist in the eyes of migratory birds. Cryptochromes,[48−51] a class of photoreceptor proteins, were proposed as the host molecules for the crucial radical pair cofactors that putatively act as a primary magnetoreceptor.[23] Cryptochrome is a signaling protein found in a wide variety of plants and animals.[48−50] Its role

Received: July 27, 2011
Revised: November 28, 2011
Published: December 15, 2011

varies widely among organisms, from the entrainment of circadian rhythms in vertebrates to the regulation of hypocotyl elongation and anthocyanin production in plants.[52−54] It has recently been demonstrated, using UV/visible transient absorption and electron paramagnetic resonance spectroscopy,[55,56] that vertebrate cryptochromes form long-lived radical pairs, involving a flavin radical and a radical derived from a redox-active amino acid. This observation demonstrates that cryptochrome harbors the type of radical pair needed for magnetic compass action and suggests that cryptochromes, through S ↔ T interconversion, are influenced by an external magnetic field. Radical pairs seen in DNA photolyase,[57−63] a light sensitive DNA repair enzyme closely related to cryptochrome, support the observation[55,56] in cryptochrome; indeed a recent study[59] demonstrated a magnetic field effect in DNA photolyase, suggesting a similar effect to exist in cryptochrome.

It has been verified that cryptochromes exist in the eyes of migratory birds[55,64−67] and that at least some cryptochrome-containing cells within the retina are active at night when the birds perform magnetic orientation in the laboratory.[64,67] Furthermore, a distinct part of the forebrain, which primarily processes input from the eyes, is highly active at night in night-migratory garden warblers (*Sylvia borin*) and European robins (*Erithacus rubecula*).[33,68−71] In summary, many findings are consistent with the hypothesis that magnetic compass detection in migratory birds takes place in the eye[33,72−76] and that cryptochromes are the primary magnetoreceptors. However, despite the success of these findings, a completely satisfactory description of the mechanism of the magnetic field effect in cryptochrome is still missing.

The process of cryptochrome photoactivation was discussed earlier, and several reaction schemes were proposed.[57,66,77−80] However, the proposed schemes are incomplete, usually accounting for only some of several observations. Cryptochrome binds internally the chromophore flavin adenine dinucleotide (FAD).[50,66,77,79−82] At least in plant cryptochromes from *Arabidopsis thaliana*[55,77−79,83,84] blue light leads to conversion of the fully oxidized FAD to the semireduced $FADH^{\bullet}$ form, the latter representing the signaling state. The conversion happens in the course of a light-induced electron transfer reaction involving FAD and a chain of three tryptophan amino acids that bridge the space between FAD and the protein surface,[55,56,85] as illustrated in Figure 1. Atomic level structures of plant cryptochrome are known for *Arabidopsis thaliana* cryptochrome-1[81] and *Arabidopsis thaliana* DASH-type cryptochrome-3.[82] In cryptochromes from insects, light excitation leads to the formation of a flavin anion radical, $FAD^{\bullet-}$.[84,86] It is currently under debate whether the anion radical represents the signaling state or whether it is only a functionally insignificant short-lived intermediate.[80,86,87] The difference in the photocycles of plant and insect cryptochromes illustrates that detailed analysis of the transient states in cryptochromes is needed in light of the fact that major variations arise between different cryptochromes, even regarding the nature of their signaling states. Such analysis can only be performed in vitro on cryptochromes extracted from specific organisms.

Unfortunately, relative to plant and insect cryptochromes, little is known at present about structure and photocycle of avian cryptochromes. Therefore, we study here a model cryptochrome from a general perspective. Our goal is to demonstrate what observations are needed for resolving photoactivation and magnetoreception of the protein. By suggesting an analysis method

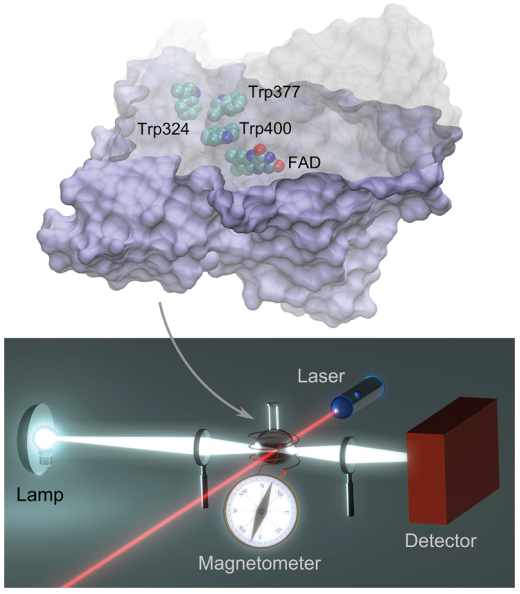

Figure 1. *Arabidopsis thaliana* cryptochrome in transient absorption experiment. (Top) The structure of cryptochrome-1 from *Arabidopsis thaliana*[81] is shown together with the highlighted flavin cofactor (FAD) and the tryptophan triad Trp400, Trp377, Trp324. (Bottom) Transient absorption of cryptochrome is probed by means of the pump−probe experiment, as described in the experiment from ref 55. The sample containing cryptochrome is irradiated with a pulsed laser beam (red) that generates a measurable concentration of excited states (FAD*) in the system. FAD* decays then to a series of intermediates back to FAD, while some of the intermediates being probed by the probe beam (white) are used to measure the absorption spectrum of transient species. Additionally, magnetic field effects in cryptochrome can be studied if the sample is subjected to an external magnetic field.

that deduces from experimental observations a reaction scheme, it is our hope that further physicochemical experiments will be initiated on cryptochrome photoactivation that ultimately pinpoint the complete photoreaction and signaling process in cryptochrome and, in particular, establish when and why the anionic, $FAD^{\bullet-}$, and the neutral, $FADH^{\bullet}$, radicals are formed.

One can safely state that, in spite of numerous experimental observations of intermediate states in cryptochrome, the actual photoreaction is still not fully understood.[55−57,66,77−79,84,88−91] Figure 2 shows a scheme of cryptochrome activation and inactivation. The scheme incorporates the key observation that the flavin cofactor in cryptochrome is observed in three interconvertible redox forms, FAD, $FADH^{\bullet}$, and $FADH^{-}$.[56,57,77,83,89,92] In this scheme, the FAD form is inactive (nonsignaling) and accumulates to a high level in the dark.[77−80,88] Blue light triggers photoreduction of FAD to establish a photoequilibrium that favors $FADH^{\bullet}$ over FAD or $FADH^{-}$.[77−80,88] As pointed out above, in plant cryptochromes, signaling is linked to the formation of the $FADH^{\bullet}$ state. This state can absorb a second, blue-green light photon in which case $FADH^{\bullet}$ is converted to the fully reduced, inactive form $FADH^{-}$: the latter reoxidizes in the dark to the original FAD resting state.[25,57,59,77,89,92]

The tryptophan triad in cryptochrome, depicted in Figure 1, is crucial for the functioning of the protein as a primary electron donor.[55,56,78] In *Arabidopsis thaliana*, the triad consists of Trp324, Trp377, and Trp400 as shown in Figure 1. In cryptochromes from garden warbler (*Sylvia borin*),[55] *Drosophila melanogaster*,[56,79,80] and *Homo sapiens*,[56,79] the tryptophan-triad

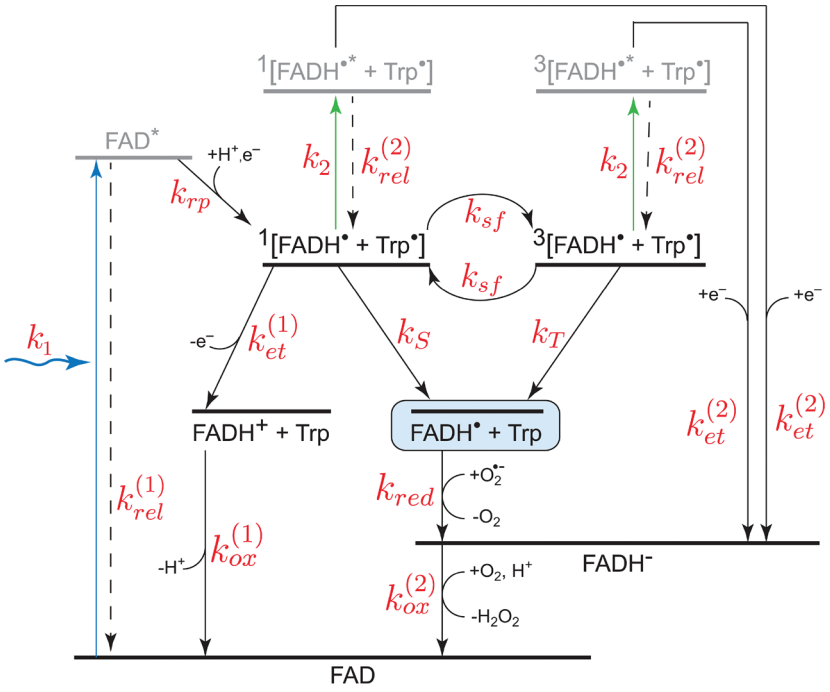

Figure 2. Cryptochrome activation and inactivation reactions. Cryptochrome is activated through absorbing a blue-light photon by the flavin cofactor, responsible for protein's signaling. Initially, the flavin cofactor in cryptochrome is present in its fully oxidized FAD state. After absorbing a photon, FAD becomes promoted to an excited FAD* state. FAD* is then protonated and receives an electron from a nearby tryptophan (see Figure 1), leading to the formation of the [FADH$^\bullet$ + Trp$^\bullet$] radical pair, which exists in singlet and triplet overall electron spin states, denoted as $^1[\cdots]$ and $^3[\cdots]$, respectively. The Trp$^\bullet$ radical may receive an additional electron from a nearby tyrosine[55,78] or become deprotonated,[24,95] quenching the radical pair and fixing the electron on the FADH$^\bullet$ cofactor. Under aerobic conditions, FADH$^\bullet$ slowly reverts back to the initial inactive FAD state through the also inactive FADH$^-$ state of the flavin cofactor. Before the [FADH$^\bullet$ + Trp$^\bullet$] radical pair in cryptochrome is quenched, the electron of the FADH$^\bullet$ radical can back-transfer to the Trp$^\bullet$ radical, thereby also ending the signaling state of the protein. The electron back-transfer leads to the formation of FADH$^+$ and can only occur if the spins of the two unpaired electrons in the radical pair [FADH$^\bullet$ + Trp$^\bullet$] are in an overall singlet state. While the flavin cofactor is in its FADH$^\bullet$ state, cryptochrome may absorb a second blue-green photon, thereby transferring it into a nonsignaling state with the flavin cofactor in the FADH$^-$ conformation.

is conserved.[24,55−57] Before light activation, the flavin cofactor of cryptochrome is present in its fully oxidized FAD state (see Figure 2). FAD absorbs blue light, being thereby promoted to an excited state, FAD*, which is then protonated, likely from a nearby aspartic acid[93] and receives an electron from the nearby tryptophan (see Figure 1), leading to the formation of a [FADH$^\bullet$ + Trp400$^\bullet$] radical pair.[24] This radical pair is further transformed into a [FADH$^\bullet$ + Trp324$^\bullet$] radical pair (denoted in Figure 2 as ^{1,3}[FADH$^\bullet$ + Trp$^\bullet$]) via sequential electron transfer, also called paramagnetic−diamagnetic exchange,[94] involving the tryptophan triad chain.[24,56,57] The [FADH$^\bullet$ + Trp$^\bullet$] radical pair exists in singlet and triplet states, denoted in Figure 2 as ^{1}[FADH$^\bullet$ + Trp$^\bullet$] and ^{3}[FADH$^\bullet$ + Trp$^\bullet$], respectively.

The [FADH$^\bullet$ + Trp$^\bullet$] radical pair is associated with the cryptochrome signaling state since it involves the flavin cofactor in the FADH$^\bullet$ redox state. We note, though, that the semiquinone FADH$^\bullet$ state of FAD was identified as the signaling state in plant cryptochrome from *Arabidopsis thaliana*[77,83,84] but that the signaling state of avian cryptochrome is still unknown. In our study, we generalize the observation in *Arabidopsis thaliana* to birds; if future studies will demonstrate that a different redox state of the flavin cofactor is governing the signaling behavior of avian cryptochromes, the suggested scheme can be readily adapted. We also note that the Trp$^\bullet$ radical may receive an additional electron from a nearby tyrosine[55,78] or become deprotonated,[24,95] stabilizing the FADH$^\bullet$ redox state. The charge state of the tryptophan radical in the radical pair state might be crucial for the energetics and kinetics of the reaction pathway, but it is not essential in a methodological sense, the main focus of the present study. The lifetime of the radical pair state [FADH$^\bullet$ + Trp$^\bullet$] in cryptochrome is $\gtrsim 6\,\mu$s, according to transient EPR measurement.[56]

Under aerobic conditions, the FADH$^\bullet$ redox state reverts back to the initial FAD state[55,77,78,92] (see Figure 2). This process is not well understood but seems to occur on a millisecond time scale.[55,77,78] It has been suggested that the back-reaction involves the superoxide radical $O_2^{\bullet-}$,[43] the reaction evolving through the inactive FADH$^-$ state of the flavin cofactor,[25,43,96] as depicted in Figure 2. The lifetime of the FADH$^-$ state, populated such, should be long enough to allow its detection in transient absorption measurements.[55,56]

Quenching of the [FADH$^\bullet$ + Trp$^\bullet$] radical pair in cryptochrome can also arise through electron back-transfer from FADH$^\bullet$ to a tryptophan. This back-transfer, leading to formation of FADH$^+$ (see Figure 2), can only occur if the spins of the two unpaired electrons are in an overall singlet state. An external magnetic field can influence the overall electron spin state through the Zeeman interaction acting jointly with hyperfine coupling with hydrogen and nitrogen atoms.[24,25,37,45] If the overall electron spin state of [FADH$^\bullet$ + Trp$^\bullet$] is triplet, electron back-transfer and formation of FADH$^+$ cannot occur, extending the time cryptochrome stays in its signaling state. The FADH$^+$ state has a short lifetime and decays quickly to the fully oxidized FAD configuration via deprotonation.

According to recent experimental measurements[57,77,79,88] and as pointed out above, cryptochrome may absorb an additional blue-green light photon, thereby transferring itself into a non-signaling state, namely, with the flavin cofactor in the $FADH^-$ redox state. The process involves the transition $FADH^\bullet \rightarrow FADH^{\bullet *} \rightarrow FADH^-$, depicted in Figure 2. After excitation, the flavin cofactor in the $FADH^{\bullet *}$ conformation has an electron vacancy, allowing it to accept an electron from a nearby tryptophan and, thereby, be transformed into $FADH^-$. In order to stabilize $FADH^-$, the terminating tryptophan of the triad should be in its radical state. In the absence of such tryptophan radical prior to $FADH^\bullet$ excitation, the excited electron in $FADH^{\bullet *}$ will back-transfer to the electron vacancy in tryptophan as soon as $FADH^-$ is formed.

If cryptochrome is indeed the avian magnetoreceptor protein, its signaling state is expected to be sensitive to a magnetic field, the latter controlling the lifetime of the $FADH^\bullet$ state. In earlier studies, we demonstrated that weak magnetic fields, comparable with the geomagnetic field, can alter the lifetime of $FADH^\bullet$ by 5−10%.[24,25] In these earlier studies, we considered reactions in isolation, while in the present study, we investigate the complete activation cycle. In the following, we suggest a light-driven reaction cycle in cryptochrome that exhibits a representative magnetic field effect on the signaling state of the protein. The reaction cycle is supported by transient absorption and electron-spin-resonance observations[55,56] and incorporates known attributes of avian magnetoreception. We demonstrate how the proposed reaction cycle can be compared to experiment.

METHODS

Cryptochrome is a sensory protein.[56,66,77,79,88,89] Its relevant properties, namely, light activation and deactivation, arise through a complex reaction scheme linking many intermediate states. In the case of magnetoreception, cryptochrome activation and deactivation is apparently magnetic field dependent. The long-range goal of our study is to establish cryptochrome's photoreaction scheme unequivocally, combining measurement and theoretical analysis.

The key for the stated goal are measurements of cryptochrome transient photoabsorption[55,56] that presently suggest different reaction schemes, consistent with the same experimental observations. For the sake of concreteness, we single out one reaction scheme, namely, the one shown in Figure 2. We will demonstrate how this scheme can be reconciled with observed time-dependent absorption spectra. The method can be applied to variant schemes, too.

The efficiency of light absorption at wavelength λ by an absorbing medium is characterized through the absorbance $A(\lambda)$ defined as[97]

$$A(\lambda) = d \sum_{i=1}^{N} \varepsilon_i(\lambda) c_i \tag{1}$$

where N is the number of different light-absorbing components in the system with the concentrations c_i (expressed in $\mathrm{mol \cdot L^{-1}}$) and the molar absorption (extinction) coefficients $\varepsilon_i(\lambda)$ (in $\mathrm{L \cdot mol^{-1} cm^{-1}}$); d is the thickness of the absorbing medium (in cm). The molar absorption coefficients in eq 1 are wavelength-dependent, resulting in a wavelength-dependence of the sample absorbance. The time evolution of the intermediate states concentrations can be calculated from the set of coupled kinetic equations

$$\frac{d[FAD]}{dt} = -k_1[FAD] + k_{rel}^{(1)}[FAD^*] + k_{ox}^{(1)}[FADH^+] + k_{ox}^{(2)}[FADH^-] \tag{2}$$

$$\frac{d[FAD^*]}{dt} = k_1[FAD] - k_{rp}[FAD^*] - k_{rel}^{(1)}[FAD^*] \tag{3}$$

$$\frac{d[^1(FADH^\bullet Trp^\bullet)]}{dt} = k_{rp}[FAD^*] - (k_{et}^{(1)} + k_2 + k_S + k_{sf})[^1(FADH^\bullet Trp^\bullet)] + k_{sf}[^3(FADH^\bullet Trp^\bullet)] + k_{rel}^{(2)}[^1(FADH^{\bullet *} Trp^\bullet)] \tag{4}$$

$$\frac{d[^3(FADH^\bullet Trp^\bullet)]}{dt} = k_{sf}[^1(FADH^\bullet Trp^\bullet)] - (k_2 + k_T + k_{sf})[^3(FADH^\bullet Trp^\bullet)] + k_{rel}^{(2)}[^3(FADH^{\bullet *} Trp^\bullet)] \tag{5}$$

$$\frac{d[^1(FADH^{\bullet *} Trp^\bullet)]}{dt} = k_2[^1(FADH^\bullet Trp^\bullet)] - (k_{rel}^{(2)} + k_{et}^{(2)})[^1(FADH^{\bullet *} Trp^\bullet)] \tag{6}$$

$$\frac{d[^3(FADH^{\bullet *} Trp^\bullet)]}{dt} = k_2[^3(FADH^\bullet Trp^\bullet)] - (k_{rel}^{(2)} + k_{et}^{(2)})[^3(FADH^{\bullet *} Trp^\bullet)] \tag{7}$$

$$\frac{d[FADH^+]}{dt} = k_{et}^{(1)}[^1(FADH^\bullet Trp^\bullet)] - k_{ox}^{(1)}[FADH^+] \tag{8}$$

$$\frac{d[FADH^\bullet]}{dt} = k_S[^1(FADH^\bullet Trp^\bullet)] + k_T[^3(FADH^\bullet Trp^\bullet)] - k_{red}[FADH^\bullet] \tag{9}$$

$$\frac{d[FADH^-]}{dt} = k_{red}[FADH^\bullet] + k_{et}^{(2)}([^1(FADH^{\bullet *} Trp^\bullet)] + [^3(FADH^{\bullet *} Trp^\bullet)]) - k_{ox}^{(2)}[FADH^-] \tag{10}$$

Here, square brackets denote the concentration of transient states introduced in Figure 2; [FAD], [FAD*], $[^1(FADH^\bullet Trp^\bullet)]$, $[^3(FADH^\bullet Trp^\bullet)]$, $[^1(FADH^{\bullet *} Trp^\bullet)]$, $[^3(FADH^{\bullet *} Trp^\bullet)]$, $[FADH^{\bullet *}]$, $[FADH^+]$, $[FADH^\bullet]$, and $[FADH^-]$ denote the concentration of FAD, FAD*, $^1[FADH^\bullet + Trp^\bullet]$, $^3[FADH^\bullet + Trp^\bullet]$, $^1[FADH^{\bullet *} + Trp^\bullet]$, $^3[FADH^{\bullet *} + Trp^\bullet]$, $FADH^{\bullet *}$, $FADH^+ + Trp$, $FADH^\bullet + Trp$, and $FADH^-$ states, respectively. The rate constants k_1, k_2, k_{rp}, k_{sf}, k_S, k_T, $k_{rel}^{(1)}$, $k_{rel}^{(2)}$, $k_{ox}^{(1)}$, $k_{ox}^{(2)}$, k_{red}, $k_{et}^{(1)}$, and $k_{et}^{(2)}$ in eqs 2−10 capture the different processes underlying cryptochrome photoactivation and relaxation shown in Figure 2, assuming all processes can be described through first order kinetics.

Table 1. Rate Constants of Various Kinetic Processes in Cryptochrome[a]

rate constant	physical process	characteristic time	rate (s^{-1})	source
k_1	FAD excitation by blue light	1.47 ns	6.8×10^8	estimate; see Supporting Information
k_2	$FADH^\bullet$ excitation by green light	1.1 ns	9×10^8	estimate; see Supporting Information
k_{rp}	$^1[FADH^\bullet + Trp^\bullet]$ radical pair formation	30 ps	3.3×10^{10}	experiment[63]
k_{sf}	singlet ↔ triplet interconversion	1 μs	10^6	estimate[27]
k_S	singlet state decay	10 μs	10^5	consistent with ref 56
k_T	triplet state decay	10 μs	10^5	consistent with ref 56
$k_{rel}^{(1)}$	FAD* relaxation to FAD	80 ps	1.25×10^{10}	experiment[60]
$k_{rel}^{(2)}$	$FADH^{\bullet *}$ relaxation to $FADH^\bullet$	80 ps	1.25×10^{10}	experiment[60]
$k_{ox}^{(1)}$	$FADH^+$ deprotonation	10 ps	10^{11}	experiment[57,59,77,79]
$k_{ox}^{(2)}$	$FADH^-$ oxidation	4 ms	250	experiment[55]
k_{red}	$FADH^\bullet$ reduction	14 ms	70	experiment[55]
$k_{et}^{(1)}$	electron transfer $FADH^\bullet \rightarrow Trp^\bullet$	10 μs	10^5	experiment[56]
$k_{et}^{(2)}$	electron transfer $Trp \rightarrow FADH^{\bullet *}$	38 ps	2.6×10^{10}	experiment[60]

[a] Characteristic time scales and rate constants for the kinetic processes in cryptochrome as depicted in Figure 2.

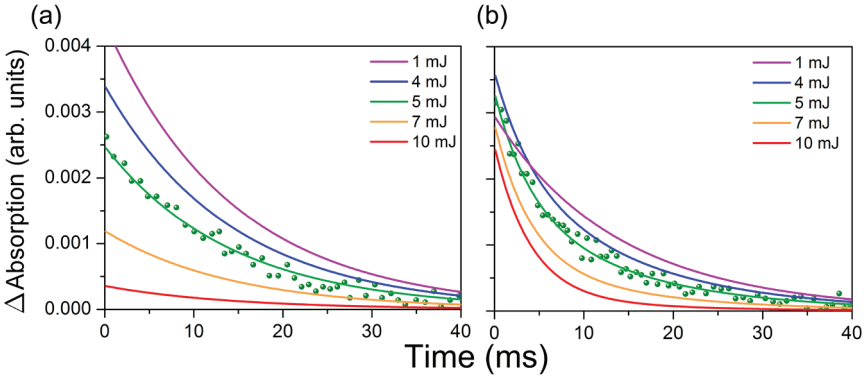

Figure 3. Cryptochrome transient absorption spectra. Time profiles of the change in the transient absorption spectra from the absorbance to prior laser excitation of the sample calculated for cryptochrome excited by laser pulses of different intensity (see Figure 1), for the probe-beam of wavelengths 550−630 nm (plot a), and 490−550 nm (plot b). The laser pulse duration chosen was 5 ns as in the experiment of ref 55 at 355 nm wavelength. The energies of the pulse used in the calculation are indicated in the inset. The wavelengths used in the calculation were chosen consistent with the experimental measurements of the transient absorption spectra in garden warbler cryptochrome.[55] Dots correspond to the experimentally measured data recorded for the pulse energy of 5 mJ.[55]

The choice of the appropriate rate constants is discussed in the Supporting Information and is summarized in Table 1.

To demonstrate that the reaction scheme in Figure 2 is consistent with observed cryptochrome transient absorption,[55] we evaluate the time development of [FAD], [FAD*], [^{1}($FADH^\bullet$ $Trp^\bullet$)], [^{3}($FADH^\bullet Trp^\bullet$)], [^{1}($FADH^{\bullet *} Trp^\bullet$)], [^{3}($FADH^{\bullet *} Trp^\bullet$)], [$FADH^{\bullet *}$], [$FADH^+$], and [$FADH^-$]. The evaluation can be achieved by numerical integration of the rate eqs 2−10. We assume the initial condition holds $[FAD]|_{t=0} = c_0$, while all other intermediate states are unpopulated. c_0 is the initial ($t = 0$) concentration of cryptochrome in the sample before excitation by a laser pulse. According to the experimental study,[55] c_0 is held at 20 μM.

RESULTS

In the following, the time-dependence of the transient absorption in cryptochrome is studied for the reaction scheme shown in Figure 2. The calculated transient absorption spectra based on the scheme are then compared to available experimental data. After the postulated reaction has been validated through comparison with experimental observations, the influence of an external magnetic field on the signaling state of the protein is analyzed.

Light Intensity Dependence of Transient Spectra. To probe the transient states in cryptochrome, a cryptochrome-containing sample from the retina of garden warbler had been studied.[55] The transient absorption was measured using the pump−probe experiment depicted in Figure 1, where a Nd:YAG laser operating at 355 nm excited the sample, and a 150 W tungsten lamp was used for monitoring reaction intermediates. To study the transient states in cryptochrome during its photoactivation cycle, the wavelength of the probe beam was adjusted to allow absorption of either the $FADH^-$ and $FADH^\bullet$ states of the flavin cofactor (absorbing at 490−550 nm) or of the $FADH^\bullet$ state only (absorbing at 550−630 nm). The experimentally recorded time profiles of the transient absorption spectra for the two regimes are shown in Figure 3. As discussed in the report of the experiment,[55] transient absorption observed at 490−550 nm reveals a double exponential decay with decay times of (4 ± 1) ms and (14 ± 1) ms, whereas transient absorption at 550−630 nm shows only a single exponential decay with a decay time of (14 ± 1) ms. The decay times,

therefore, may be attributed to $FADH^{\bullet}$ (14 ms) and $FADH^{-}$ (4 ms). The experimental error of the decay times is not provided in the original experimental papers and has been estimated here by digitizing the experimental data points and fitting the absorption curves with single and double exponential decays.

According to the original explanation of the recorded absorption patterns,[55] the double exponential decay of the transient absorption spectrum was attributed to the presence of the tryptophan radical in the sample for over 4 ms and to the protein's signaling state associated with $FADH^{\bullet}$ to be lasting over 14 ms. This explanation implies a radical pair lifetime in cryptochrome of over 1 ms, which is unusually long. However, a lifetime of the radical pair beyond 10 μs would abolish a magnetic field effect as singlet and triplet radical pair states $^1[FADH^{\bullet} + Trp^{\bullet}]$ and $^3[FADH^{\bullet} + Trp^{\bullet}]$, respectively, would then be dominated by electron spin relaxation that occurs faster than 10 μs.[27] For a significant magnetic field effect to arise, the radical pair lifetime needs to be short compared to electron spin relaxation times and, in fact, needs to be comparable with hyperfine interaction-induced singlet−triplet interconversion times of 1 μs.[27] At present there is no physical mechanism known that could explain a magnetic field effect for radical pair lifetimes >10 μs. The many suggestions for cryptochrome involvement in magnetoreception, for example, the finding of Reppert et al. for a cryptochrome knockout mutant of fruit flies,[98,99] suggests to further pursue the possibility of a cryptochrome-based biochemical compass tied likely to a radical pair lifetime of <10 μs.

Such short lifetime seems to contradict the finding of Brettel et al.[78] who isolated cryptochrome-1 from *Arabidopsis thaliana* and studied the transient absorption of the protein; analyzing the change of the transient absorption, the authors suggest that a tryptophan radical is present in cryptochrome for over 1 ms. However, this result cannot be applied to the present case since Brettel et al. studied plant cryptochrome instead of avian cryptochrome. Although the photocycle of the members of the cryptochrome family should exhibit similarity, experiments show great variation between cryptochromes extracted from different organisms.[77,80,83,84,86,87] Furthermore, the change in the transient absorption spectra attributed by Brettel et al. to the presence of the tryptophan radical may stem from another cryptochrome component with similar absorption properties. To explain an error due to such component, we note that cryptochrome transient absorption relative to the absorbance prior to laser excitation can be calculated using eq 1, where the summation is performed over the FAD, $FADH^{-}$, and $FADH^{\bullet}$ states for a 490−550 nm probe-beam and includes only one term corresponding to the $FADH^{\bullet}$ state in the case of a 550−630 nm probe-beam. In the suggested model, the transient $^1[FADH^{\bullet} + Trp^{\bullet}]$ and $^3[FADH^{\bullet} + Trp^{\bullet}]$ states have no noticeable influence on the absorption spectrum since the lifetime of these radical pair states is assumed to be several orders of magnitude shorter than the lifetime of the $FADH^{-}$ and $FADH^{\bullet}$ states. If the lifetime of the radical pair state is on the order of milliseconds, as suggested in ref 55, then the absorbance of the tryptophan radical becomes important.

Figure 3 shows the calculated time-dependence of the transient absorption in cryptochrome, obtained from solving rate eqs 2−10, for wavelengths at 490−550 nm and 550−630 nm. The figure shows that the energy of the laser pulse impacts the absorption properties of the protein. The dependence on the laser-pulse energy is due to the rate constant k_2, which is proportional to the laser pulse power (see Supporting Information for more details). The transient absorption spectrum calculated for a pulse power of 1 MW, i.e., corresponding to the experimental 5 ns pulse carrying 5 mJ energy, can be compared to the experimental result reported earlier.[55] As can be seen in Figure 3, the calculated transient absorption perfectly matches the recorded data for a 490−550 nm and a 550−630 nm probe-beam.

Increasing the energy of the laser pump-pulse enhances the rate constant k_2 leading to faster population of the $FADH^{-}$ state (see Figure 2). This enhancement can be verified experimentally since the $FADH^{-}$ and $FADH^{\bullet}$ states in cryptochrome absorb light differently. Indeed, exciting the cryptochrome-containing sample with a pulse of higher intensity should lead to diminished absorption at 550−630 nm and a single exponential decay at 490−550 nm with a decay time of 4 ms. Figure 3 illustrates how the time-dependence of the transient absorption behaves once the intensity of the pump pulse is increased.

A decrease of the pump-pulse power leads to suppression of the $FADH^{\bullet} \rightarrow FADH^{\bullet *} \rightarrow FADH^{-}$ channel and extends the lifetime of the $[FADH^{\bullet} + Trp^{\bullet}]$ radical pair. Figure 3 shows the dependence of the transient absorption calculated for the laser pulse energy of 1 mJ acting over 5 ns. For such weak and short pulse, the transition $FADH^{\bullet} \rightarrow FADH^{\bullet *} \rightarrow FADH^{-}$ is significantly suppressed as the redistribution of the $FADH^{\bullet}$ concentration toward the $FADH^{-}$ state is quenched. Figure 3 shows that for lower light intensities, the absolute magnitude of the absorption at 550−630 nm increases because the concentration of the $FADH^{\bullet}$ states increases. Figure 3 presents experimental data only for laser pulse energy of 5 mJ; to establish unambiguity of the suggested model, it is necessary to perform measurement at laser pulse energies of 1, 4, 7, and 10 mJ.

It is worth noting that the photoexcitation rate constants k_1 and k_2 depend not only on the laser-pulse energy but also critically on the wavelength of the pulse and on pulse duration. Figure 4 presents the time evolution of the concentration of the transient states in cryptochrome calculated from eqs 2−10 for the photoexcitation regimes considered in one study[55] (plot a) and in another[56] (plot b). The difference in the pump-pulse leads to a significant change in the population of transient states. Thus, for a laser pulse of 5 ns duration, of 5 mJ energy, and 355 nm wavelength (see Figure 4a), the population of the $FADH^{-}$ state after 5 ns is about 5 times higher than the population of the radical pair $^1[FADH^{\bullet} + Trp^{\bullet}]$ state. The early population of the $FADH^{-}$ state readily explains both the double-exponential decay of the transient absorption spectrum at 490−550 nm and a single exponential decay at 550−630 nm as reported earlier.[55]

The absorption of the semiquinone state of the flavin radical ($FADH^{\bullet}$) at 460 nm is significantly weaker in comparison to absorption at 355 nm (see Figure S1 in Supporting Information) and, therefore, the photoexcitation rate constant k_2 at 460 nm is smaller than at 355 nm. Figure 4b shows that for a laser pulse of 6 ns duration, 4 mJ energy, and 460 nm wavelength, the population of the $FADH^{-}$ state after pulse excitation is smaller than the population of the radical pair $^1[FADH^{\bullet} + Trp^{\bullet}]$ state, arguing that the radical pair state can be better resolved at 460 nm than at 355 nm wavelength.

Influence of Magnetic Field As Seen by Transient Spectra. Comparison of measured and calculated kinetics in cryptochrome reveals good agreement and, hence, supports the reaction scheme in Figure 2. Therefore, the postulated reaction

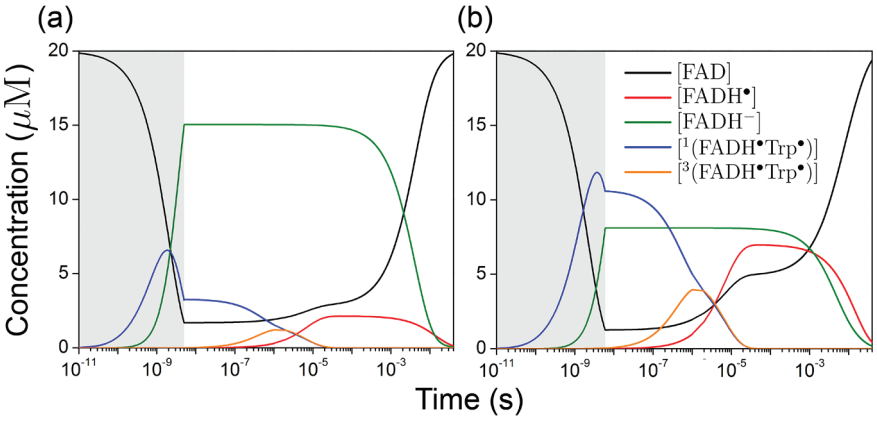

Figure 4. Population of transient states in cryptochrome. Time evolution of concentration of the transient states in cryptochrome calculated from eqs 2−10 for cryptochrome photoexcitation by a laser pulse of 5 ns duration, 5 mJ energy, and 355 nm wavelength (plot a, consistent with ref 55), and a laser pulse of 6 ns duration, 4 mJ energy, and 460 nm wavelength (plot b, consistent with ref 56). Gray areas indicate the time duration of the laser pulse.

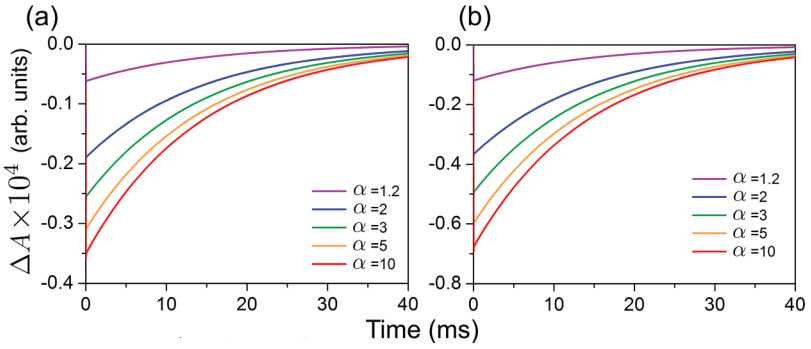

Figure 5. Magnetic field effect in cryptochrome. Change of the transient absorption spectra in cryptochrome due to a change in k_{sf} caused by an external magnetic field, calculated for the 550−630 nm probe-beam. α is defined in the text. Initial photoexcitation is due to a laser pulse of 5 ns duration, 355 nm wavelength, and 5 mJ energy (plot a) and 2.5 mJ energy (plot b). The curves $\Delta A(\alpha,t)$ in plots a and b reflect change in transient absorption due to an increased value of the k_{sf} relative to the reference value 10^6 s^{-1} (see Table 1).

scheme will be employed further to consider magnetic field effects on cryptochrome activation and deactivation.

The influence of an external magnetic field on cryptochrome photoactivation can be probed through the effect of an applied magnetic field on the transient absorption spectrum. The magnetic field influences the singlet−triplet interconversion process in cryptochrome (see Figure 2) described here extremely schematically through the first-order rate constant k_{sf}. An applied magnetic field leads to a relative change of the rate constant k_{sf},[24,25,46] which brings about an altered transient absorption. The change can be written as

$$\Delta A(\alpha, t) = A(k_{sf}, t) - A(\alpha k_{sf}, t) \qquad (11)$$

where $k_{sf} = 10^6$ s^{-1} is the reference value of the singlet−triplet interconversion rate constant (see Table 1), and α denotes the relative change in k_{sf} due to an altered magnetic field; A is defined in eq 1.

The α-value depends on several factors, such as the hyperfine interaction in the radical pair, exchange and dipole−dipole interactions, and Zeeman interaction.[24,25] An accurate calculation of α requires the solution of a stochastic Liouville equation.[24,25,46,100] We consider α-values ranging from $\alpha = 1.2$ ($k_{sf} = 1.2 \times 10^6$ s^{-1}) to $\alpha = 10$ ($k_{sf} = 10^7$ s^{-1}), thereby accounting for realistic singlet−triplet interconversion rates expected in cryptochrome when the field reorients.[24,25,27]

Deviation of α from $\alpha = 1$ can arise either through a change of magnetic field orientation or through changing field strength. The latter change can arise due to geographic variation of the geomagnetic field strength; this change is small percentage-wise but is employed by birds apparently for a so-called magnetic map sense.[101−104] In this case, detection is likely achieved by an alternative receptor, an iron-mineral-based magnetoreceptor in the beak.[104−106] The geographic variation of the magnitude of the geomagnetic field is expected to have a negligible impact on the photoreaction kinetics of cryptochrome and, therefore, is not considered here; only a change, i.e., $\alpha \neq 1$, due to reorientation in the Earth' field is considered.

For cryptochrome to exhibit a response to the change of the magnetic field direction, the protein needs be constrained orientation-wise within the organism. We have recently demonstrated that only one of three rotational degrees of freedom of cryptochrome need to be partially constrained to endow a bird with the magnetic compass.[26] Such constraint can be realized if cryptochromes are embedded in a cell membrane. The outer segment of the photoreceptor cells is an ideal structure to constrain the proteins as originally suggested in theory.[26] An experimental verification of cryptochromes localization in the outer segment of the UV photoreceptor cells was published recently.[67]

Figure 5 shows the time-dependence of ΔA for various α-values. The calculations were performed for cryptochrome

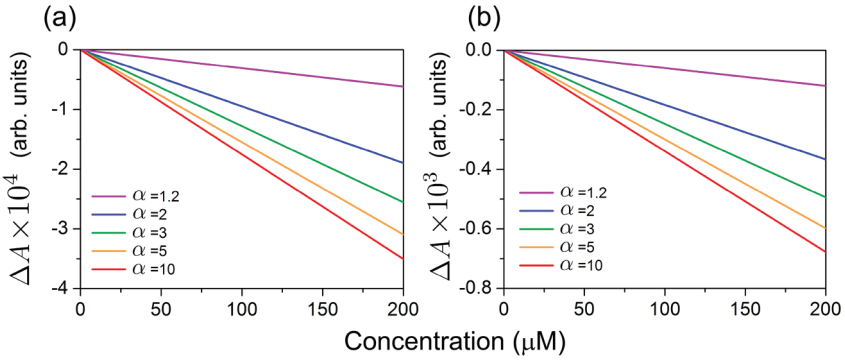

Figure 6. Magnetic field effect and probe concentration. The maximal change of the transient absorption spectra in cryptochrome calculated due to change in k_{sf} at different concentrations of protein, calculated for a 550−630 nm probe-beam. Initial photoexcitation is due to a laser pulse of 5 ns duration, 355 nm wavelength, 5 mJ energy (plot a) or 2.5 mJ energy (plot b). The curves in plots a and b show transient absorption due to an increased k_{sf} relative to the reference value of 10^6 s^{-1} (see Table 1); α is defined in the text.

photoexcitation by a laser pulse of 5 ns duration operating at 355 nm and having the energy of 5 mJ (see Figure 5a) and 2.5 mJ for which the lifetime of the $[FADH^{\bullet} + Trp^{\bullet}]$ radical pair is expected to be longer (see Figure 5b). The relative change of k_{sf} due to an applied magnetic field, α, may vary within an order of magnitude as stated above and in the Supporting Information.[24,27]

Figure 5 shows that decreasing the intensity of the pump-pulse leads to an enhancement of the magnetic field effect. The enhancement is due to the excitation channel $FADH^{\bullet} \rightarrow FADH^{\bullet *} \rightarrow FADH^{-}$ in the cryptochrome photoactivation reaction (see Figure 2), which becomes suppressed for the 2.5 mJ energy laser-pulse, such that the lifetime of the $[FADH^{\bullet} + Trp^{\bullet}]$ radical pair increases. Increasing k_{sf} ($\alpha > 1$) leads to faster singlet−triplet interconversion in the radical pair. If this interconversion becomes significantly faster than singlet and/or triplet decay, governed by rate constants k_S and k_T (see Figure 2), the magnetic field effect in cryptochrome becomes negligible, as clearly seen in Figure 5b, where the relative difference in ΔA calculated for $\alpha = 5$ and $\alpha = 10$ is small. A similar behavior is expected for higher pump-pulse intensities (see Figure 5a) at higher values of α because in this case the $[FADH^{\bullet} + Trp^{\bullet}]$ radical pair decays predominantly through the $FADH^{\bullet} \rightarrow FADH^{\bullet *} \rightarrow FADH^{-}$ channel, governed by the rate constant k_2, which is significantly larger than k_S and k_T.

The dependencies shown in Figure 5 can also be measured experimentally and are important for resolving the physical mechanism of the magnetic field effect in cryptochrome. Similar measurements were performed earlier for DNA photolyase[59] and should be repeated for cryptochrome. The time-dependence of the transient absorption change due to a magnetic field allows one not only to judge whether the protein exhibits magnetoreceptive properties but also can be used to reveal the impact of the magnetic field on the singlet−triplet interconversion rate constant k_{sf}.

Predicted absolute magnetic field effects in cryptochrome are rather small, i.e., the absorption changes only by about $(0.1-0.3) \times 10^{-4}$ for a 5 mJ pulse (see Figure 5a) and by about $(0.2-0.6) \times 10^{-4}$ for a 2.5 mJ pulse (see Figure 5b). Absolute changes of the transient absorption due to a 39 mT magnetic field in DNA photolyase were recorded to be of the order of ∼0.001,[59] e.g., larger, but still very small. The relative magnetic field effect for DNA photolyase can thus be estimated to be ∼1%. The difference in the magnetic field effect recorded for DNA photolyase and predicted now for cryptochrome is due to the concentration of DNA photolyase used in experiment,[59] which was 0.2 mM, whereas in the present study the assumed concentration of cryptochrome is only 20 μM, following an earlier study.[55] Increasing the concentration leads to an enhancement of the absolute magnetic field effect, i.e. the absolute value of the absorbance change.

In an animal, the ambient light continuously irradiates cryptochromes in the retina, and photoexcitation of $FADH^{\bullet}$ induced through strong irradiation does not arise because the rate constant k_2 becomes small as compared to the value in the transient absorption experiment. In vivo conditions lead then to an increase of the $[FADH^{\bullet} + Trp^{\bullet}]$ radical pair lifetime, increasing also the effect of an external magnetic field on cryptochrome signaling associated with $FADH^{\bullet}$.

Figure 6 shows the maximal change of the transient absorption due to a magnetic field calculated at different concentrations of the sample and at different intensities of the pump-pulse (Figure 6a for 5 mJ over 5 ns and Figure 6b for 2.5 mJ over 5 ns). The analysis in Figure 6 reveals that the magnitude of the maximal change of the transient absorption in cryptochrome increases linearly with the concentration of the sample. Thus, increasing the concentration to 200 μM could lead to an absolute magnetic field effect of about 0.0007 (see arbitrary units in Figure 6b), i.e., close to the value detected for DNA photolyase.[59] It is also worth noting that a more realistic account of the singlet−triplet interconversion predicts a relative magnetic field effect in cryptochrome of about 5−10% in a magnetic field comparable to the geomagnetic field,[24,25] which suggests that α is large, i.e. $\alpha \gg 1$, and that the reference value of k_{sf} is $\lesssim 10^6$ s^{-1}.

The expected linear concentration dependence of the maximal magnetic field effect in cryptochrome shown in Figure 6 carries important information about the rate constants in cryptochrome photoactivation reaction. In particular, the slopes of the linear dependencies shown in Figure 6 depend on these rate constants that govern the lifetime of transient states in the photoactivation reaction. The dependencies shown in Figure 6 are convenient for the experiment because the concentration of the cryptochrome-containing sample can be easily varied, and the transient absorption of the sample can then be recorded. Thus, by comparing results of the measurement with predictions of the kinetic model suggested in this article, it is feasible to justify rate constants in the photoactivation reaction and predict the lifetime of certain intermediate states in cryptochrome.

The amount of cryptochrome in the bird's retina, presently unknown, is critical for the magnitude of the magnetic field effect. For a significant signal, a cryptochrome concentration larger than 20 μM is necessary. Figures 5 and 6 allow one to draw another

important conclusion from our analysis, namely, that decreasing the intensity of the pump-pulse enhances the magnetic field effect. Interestingly, many migratory birds favor to fly at night time, i.e., when the intensity of the ambient light is low.[26]

CONCLUSIONS

Earlier investigations[23−26,45] demonstrated how a biochemical magnetic compass in birds can be realized through light-induced electron transfer reactions in cryptochrome. However, the biophysical mechanism of cryptochrome activation and signaling still remains elusive. Our study provides an important step toward resolving the mechanism of cryptochrome magnetoreception. The suggested analysis can provide a proof-of-principle whether cryptochrome is indeed the magnetoreceptor protein in birds, comparing computed kinetic data with data from transient absorption spectroscopy, as successfully applied to DNA photolyase.[59]

The results of the present calculations reveal that magnetic field effects on the absolute value of absorbance become only discernible if the concentration of the protein in the probe exceeds a critical value. Therefore, cryptochrome should be measured at different concentrations to ascertain that the minimal amount of protein is available. Transient absorption of cryptochromes at low concentration can be studied with the use of the so-called cavity-enhanced spectroscopy technique.[83] This technique traps the probe light beam in an optical cavity, containing the sample, thereby transmitting the beam through the sample multiple times and increasing the transmittance lengt, which in turn enhances the total absorption in the sample. The method permits protein concentrations below ∼1 μM,[83] resolving nevertheless small changes in the transient absorption, as they arise due to an external magnetic field. A systematic study of the dependence of the absolute absorption of a cryptochrome-containing sample on cryptochrome concentration is important for revealing the lifetime of reaction intermediates through direct comparison of experimentally recorded absorption with the prediction of the kinetic formalism suggested in this article.

The methodology suggested here illustrates how laser power, laser wavelength, laser pulse duration, probe light wavelength, and protein concentration impact measured results. In particular, we identify which measurements pinpoint the magnetoreceptive properties of cryptochrome.

The performed study assumes for its analysis reaction rate constants, which were extracted from experiment or could be estimated otherwise. The uncertainty of most of the rate constants is rather large. By measuring the transient absorption spectra in cryptochrome at different conditions, i.e., for different probe-beam intensities, different applied magnetic fields, different wavelengths of the pulse and probe beams, etc., and by comparing recorded profiles with calculated ones, one can narrow the range of consistent rate constants in the proposed reaction scheme.

Magnetoreception in birds has been found to work for light with wavelengths of up to 565−567 nm.[20,107] Thus, it is important to continue studies of cryptochrome photoactivation in vitro by maintaining the conditions close to those used in the in vivo experiments.[20,107] An important question is how the magnetic directional information is disrupted under monochromatic light of an increased intensity. It has been demonstrated that different light intensities can disorient birds in the laboratory,[18,20,108,109] and therefore, light intensity may affect the photocycle in cryptochrome. Studying transient absorption of cryptochrome in electromagnetic fields of certain frequencies, e.g., Larmor frequency of the electron,[42,43,96] is another step to link in vitro studies to behavioral investigations.[42,43]

Science is still a long way from an explanation of avian magnetoreception. The best that may be said of our understanding today is that birds indeed perceive and use magnetic field information and that their responses to magnetic fields under different conditions, light intensity and color, magnetic field strength, and presence of oscillating fields, are suggesting a complex sensory system of multiple receptors. Even if cryptochrome is confirmed as a magnetoreceptor, it remains for biologists to determine how its magnetic field modulated signaling enters into a bird's sensory perception and ultimately into its orientation behavior.

ASSOCIATED CONTENT

Supporting Information. Details on the flavin absorption spectra and discussion of the choice of rate constants in the studied reaction in cryptochrome. This material is available free of charge via the Internet at http://pubs.acs.org.

AUTHOR INFORMATION

Corresponding Author

*E-mail: ilia@illinois.edu (I.A.S.); kschulte@ks.uiuc.edu (K.S.).

ACKNOWLEDGMENT

We thank Paul Galland (University of Marburg) for providing the necessary data on flavin absorption, Robert Bittl (Freie Universität Berlin) for stimulating discussions that helped us understand the experimental aspects of the transient absorption spectroscopy, Peter Hore and colleagues (University of Oxford) for providing the necessary information on the experimental setup used in cryptochrome transient absorption experiments, and Vita Solovyeva for inspiring remarks. This work has been supported by National Science Foundation grants NSF MCB-0744057 and NSF PHY0822613 and by National Institutes of Health grant P41-RR005969. K.S. thanks the Alexander von Humboldt Foundation for support, and I.S. acknowledges support as a Beckman Fellow.

REFERENCES

(1) Mouritsen, H.; Ritz, T. *Curr. Opin. Neurobiol.* **2005**, *15*, 406–414.
(2) Wiltschko, R.; Wiltschko, W. *BioEssays* **2006**, *28*, 157–168.
(3) Solov'yov, I. A.; Schulten, K.; Greiner, W. *Phys. J.* **2010**, *9*, 23–28.
(4) Wiltschko, W.; Wiltschko, R. *Science* **1972**, *176*, 62–64.
(5) Merkel, F.; Wiltschko, W. *Vogelwarte* **1965**, *23*, 71–77.
(6) Freire, R.; Munro, U.; Rogers, L. J.; Sagasser, S.; Wiltschko, R.; Wiltschko, W. *Animal Cognition* **2008**, *11*, 547–552.
(7) Voss, J.; Keary, N.; Bischof, H. *NeuroReport* **2007**, *18*, 1053–1057.
(8) Keeton, W. *Proc. Natl. Acad. Sci. U.S.A.* **1971**, *68*, 102–106.
(9) Wiltschko, W.; Wiltschko, R. *Nature* **1981**, *291*, 433–434.
(10) Wiltschko, W.; Wiltschko, R. *Naturwissenschaften* **1998**, *85*, 164–167.
(11) Fleissner, G.; Stahl, B.; Thalau, P.; Falkenberg, G.; Fleissner, G. *Naturwissenschaften* **2007**, *94*, 631–642.
(12) Solov'yov, I. A.; Greiner, W. *Biophys. J.* **2007**, *93*, 1493–1509.
(13) Solov'yov, I. A.; Greiner, W. *Eur. Phys. J. D* **2009**, *51*, 161–172.
(14) Solov'yov, I. A.; Greiner, W. *Phys. Rev. E* **2009**, *80*, 041919–1−10.

(15) Kirschvink, J. L.; Walker, M. M.; Diebel, C. E. *Curr. Opin. Neurobiol.* **2001**, *11*, 462–467.
(16) Falkenberg, G.; Fleissner, G.; Schuchardt, K.; Kuehbacher, M.; Thalau, P.; Mouritsen, H.; Heyers, D.; Wellenreuther, G.; Fleissner, G. *PLoS One* **2010**, *5*, e9231.
(17) Wiltschko, W.; Munro, U.; Ford, H.; Wiltschko, R. *Nature* **1993**, *364*, 525–527.
(18) Wiltschko, W.; Wiltschko, R. *J. Exp. Biol.* **2001**, *204*, 3295–3302.
(19) Wiltschko, W.; Möller, A.; Gesson, M.; Noll, C.; Wiltschko, R. *J. Exp. Biol.* **2004**, *207*, 1193–1202.
(20) Muheim, R.; Bäckman, J.; Åkesson, S. *J. Exp. Biol.* **2002**, *205*, 3845–3856.
(21) Wiltschko, R.; Munro, U.; Ford, H.; Stapput, K.; Wiltschko, W. *J. Exp. Biol.* **2008**, *211*, 3344–3350.
(22) Schulten, K.; Swenberg, C. E.; Weller, A. *Z. Phys. Chem.* **1978**, *NF111*, 1–5.
(23) Ritz, T.; Adem, S.; Schulten, K. *Biophys. J.* **2000**, *78*, 707–718.
(24) Solov'yov, I. A.; Chandler, D.; Schulten, K. *Biophys. J.* **2007**, *92*, 2711–2726.
(25) Solov'yov, I. A.; Schulten, K. *Biophys. J.* **2009**, *96*, 4804–4813.
(26) Solov'yov, I. A.; Mouritsen, H.; Schulten, K. *Biophys. J.* **2010**, *99*, 40–49.
(27) Rodgers, C. T.; Hore, P. J. *Proc. Natl. Acad. Sci. U.S.A.* **2009**, *106*, 353–360.
(28) Salikhov, K.; Molin, Y.; Sagdeev, R.; Buchanenko, A. *Spin Polarization and Magnetic Field Effects in Radical Reactions*; Elsevier: Budapest, Hungary, 1984; Vol. 22.
(29) Steiner, U.; Ulrich, T. *Chem. Rev.* **1989**, *89*, 51–147.
(30) Beason, R.; Semm, P. *J. Exp. Biol.* **1996**, *199*, 1241–1244.
(31) Wiltschko, W.; Munro, U.; Ford, H.; Wiltschko, R. *Proc. R. Soc. Lond. B.* **2009**, *276*, 2227–223.
(32) Wiltschko, W.; Munro, U.; Beason, R.; Ford, H.; Wiltschko, R. *Experientia* **1994**, *50*, 679–700.
(33) Zapka, M.; Heyers, D.; Hein, C. M.; Engels, S.; Schneider, N.-L.; Hans, J.; Weiler, S.; Dreyer, D.; Kishkinev, D.; Wild, J. M.; Mouritsen, H. *Nature* **2009**, *461*, 1274–1277.
(34) Schulten, K.; Weller, A. *Biophys. J.* **1978**, *24*, 295–305.
(35) Schulten, K.; Wolynes, P. G. *J. Chem. Phys.* **1978**, *68*, 3292–3297.
(36) Schulten, K. In *Biological Effects of Static and Extremely Low Frequency Magnetic Fields*; Bernhard, J. H., Ed.; MMV Medizin Verlag: Munich, Germany, 1986; pp 133−140.
(37) Schulten, K.; Staerk, H.; Weller, A.; Werner, H.-J.; Nickel, B. *Z. Phys. Chem.* **1976**, *NF101*, 371–390.
(38) Schulten, K. *J. Chem. Phys.* **1984**, *80*, 3668–3679.
(39) Werner, H.-J.; Schulten, K.; Weller, A. *Biochim. Biophys. Acta* **1978**, *502*, 255–268.
(40) Thalau, P.; Ritz, T.; Stapput, K.; Wiltschko, R.; Wiltschko, W. *Naturwissenschaften* **2005**, *92*, 86–90.
(41) Keary, N.; Ruploh, T.; Voss, J.; Thalau, P.; Wiltschko, R.; Wiltschko, W.; Bischof, H.-J. *Front. Zool.* **2009**, *6*, 25.
(42) Ritz, T.; Thalau, P.; Phillips, J. B.; Wiltschko, R.; Wiltschko, W. *Nature* **2004**, *429*, 177–180.
(43) Ritz, T.; Wiltschko, R.; Hore, P.; Rodgers, C. T.; Stapput, K.; Thalau, P.; Timmel, C. R.; Wiltschko, W. *Biophys. J.* **2009**, *96*, 3451–3457.
(44) Wiltschko, R.; Stapput, K.; Ritz, T.; Thalau, P.; Wiltschko, W. *HFSP J.* **2007**, *1*, 41–48.
(45) Solov'yov, I. A.; Chandler, D. E.; Schulten, K. *Plant Signaling Behavior* **2008**, *3*, 676–677.
(46) Cintolesi, F.; Ritz, T.; Kay, C.; Timmel, C.; Hore, P. *Chem. Phys.* **2003**, *294*, 707–718.
(47) Maeda, K.; Henbest, K. B.; Cintolesi, F.; Kuprov, I.; Rodgers, C. T.; Liddell, P. A.; Gust, D.; Timmel, C. R.; Hore, P. J. *Nature* **2008**, *453*, 387–390.
(48) Ahmad, M.; Cashmore, A. R. *Plant Mol. Biol.* **1996**, *30*, 851–861.
(49) Cashmore, A. R.; Jarillo, J. A.; Wu, Y.-J.; Liu, D. *Science* **1999**, *284*, 760–765.
(50) Sancar, A. *Chem. Rev.* **2003**, *103*, 2203–2237.
(51) Ahmad, M.; Cashmore, A. *Nature* **1993**, *366*, 162–166.
(52) Lin, C.; Todo, T. *Gen. Biol.* **2005**, *6*, 220.1–220.9.
(53) Partch, C. L.; Sancar, A. *Methods Enzymol.* **2005**, *393*, 726–745.
(54) Christie, J. M.; Briggs, W. R. *J. Biol. Chem.* **2001**, *276*, 11457–11460.
(55) Liedvogel, M.; Maeda, K.; Henbest, K.; Schleicher, E.; Simon, T.; Timmel, C. R.; Hore, P.; Mouritsen, H. *PLoS One* **2007**, *2*, e1106.
(56) Biskup, T.; Schleicher, E.; Okafuji, A.; Link, G.; Hitomi, K.; Getzoff, E. D.; Weber, S. *Angew. Chem., Int. Ed.* **2009**, *48*, 404–407.
(57) Kao, Y.-T.; Tan, C.; Song, S.-H.; Öztürk, N.; Li, J.; Wang, L.; Sancar, A.; Zhong, D. *J. Am. Chem. Soc.* **2008**, *130*, 7695–7701.
(58) Prytkova, T. R.; Beratan, D. N.; Skourtis, S. S. *Proc. Natl. Acad. Sci. U.S.A.* **2007**, *104*, 802–807.
(59) Henbest, K. B.; Maeda, K.; Hore, P. J.; Joshi, M.; Bacher, A.; Bittl, R.; Weber, S.; Timmel, C. R.; Schleicher, E. *Proc. Natl. Acad. Sci. U.S.A.* **2008**, *105*, 14395–14399.
(60) Byrdin, M.; Eker, A. P.; Vos, M. H.; Brettel, K. *Proc. Natl. Acad. Sci. U.S.A.* **2003**, *100*, 8676–8681.
(61) Gindt, Y. M.; Vollenbroek, E.; Westphal, K.; Sackett, H.; Sancar, A.; Babcock, G. T. *Biochem.* **1999**, *38*, 3857–3866.
(62) Aubert, C.; Mathis, P.; Eker, A. P.; Brettel, K. *Proc. Natl. Acad. Sci. U.S.A.* **1999**, *96*, 5423–5427.
(63) Aubert, C.; Vos, M. H.; Mathis, P.; Eker, A. P.; Brettel, K. *Nature* **2000**, *405*, 586–590.
(64) Mouritsen, H.; Janssen-Bienhold, U.; Liedvogel, M.; Feenders, G.; Stalleicken, J.; Dirks, P.; Weiler, R. *Proc. Natl. Acad. Sci. U.S.A.* **2004**, *101*, 14294–14299.
(65) Möller, A.; Sagasser, S.; Wiltschko, W.; Schierwater, B. *Naturwissenschaften* **2004**, *91*, 585–588.
(66) Liedvogel, M.; Mouritsen, H. *J. R. Soc. Interface* **2010**, *7*, S147–S162.
(67) Nießner, C.; Denzau, S.; Gross, J. C.; Peichl, L.; Bischof, H.-J.; Fleissner, G.; Wiltschko, W.; Wiltschko, R. *PLoS ONE* **2011**, *6*, e20091.
(68) Mouritsen, H.; Feenders, G.; Liedvogel, M.; Wada, K.; Jarvis, E. *Proc. Natl. Acad. Sci. U.S.A.* **2005**, *102*, 8339–8344.
(69) Liedvogel, M.; Feenders, G.; Wada, K.; Troje, N.; Jarvis, E.; Mouritsen, H. *Eur. J. Neurosci.* **2007**, *25*, 1166–1173.
(70) Feenders, G.; Liedvogel, M.; Rivas, M.; Zapka, M.; Horita, H.; Hara, E.; Wada, K.; Mouritsen, H.; Jarvis, E. *PLoS One* **2008**, *3*, e1768.
(71) Heyers, D.; Manns, M.; Luksch, H.; Güntürkün, O.; Mouritsen, H. *PLoS One* **2007**, *2*, e937.
(72) Hein, C. M.; Zapka, M.; Heyers, D.; Kutzschbauch, S.; Schneider, N.-L.; Mouritsen, H. *J. R. Soc. Interface* **2010**, *7*, S227–S233.
(73) Wiltschko, W.; Traudt, J.; Güntürkün, O.; Prior, H.; Wiltschko, R. *Nature* **2002**, *419*, 467–470.
(74) Hein, C. M.; Engels, S.; Kishkinev, D.; Mouritsen, H. *Nature* **2011**, *471*, E11–E12.
(75) Wiltschko, W.; Traudt, J.; Güntürkün, O.; Prior, H.; Wiltschko, R. *Nature* **2011**, *471*, E12–E13.
(76) Stapput, K.; Güntürkün, O.; Hoffmann, K.-P.; Wiltschko, R.; Wiltschko, W. *Curr. Biol.* **2010**, *20*, 1259–1262.
(77) Bouly, J.-P.; Schleicher, E.; Dionisio-Sese, M.; Vandenbussche, F.; Van Der Straeten, D.; Bakrim, N.; Meier, S.; Batschauer, A.; Galland, P.; Bittl, R.; Ahmad, M. *J. Biol. Chem.* **2007**, *282*, 9383–9391.
(78) Giovani, B.; Byrdin, M.; Ahmad, M.; Brettel, K. *Nat. Struct. Biol.* **2003**, *10*, 489–490.
(79) Hoang, N.; Schleicher, E.; Kacprzak, S.; Bouly, J.-P.; Picot, M.; Wu, W.; Berndt, A.; Wolf, E.; Bittl, R.; Ahmad, M. *PLoS Biol.* **2008**, *6*, 1559–1569.
(80) Shirdel, J.; Zirak, P.; Penzkofer, A.; Breitkreuz, H.; Wolf, E. *Chem. Phys.* **2008**, *352*, 35–47.
(81) Brautigam, C. A.; Smith, B. S.; Ma, Z.; Palnitkar, M.; Tomchick, D. R.; Machius, M.; Deisenhofer, J. *Proc. Natl. Acad. Sci. U.S.A.* **2004**, *101*, 12142–12147.

(82) Pokorny, R.; Klar, T.; Hennecke, U.; Carell, T.; Batschauer, A.; Essen, L.-O. *Proc. Natl. Acad. Sci. U.S.A.* **2008**, *105*, 21023–21027.
(83) Banerjee, R.; Schleicher, E.; Meier, S.; Viana, R. M.; Pokorny, R.; Ahmad, M.; Bittl, R.; Batschauer, A. *J. Biol. Chem.* **2007**, *282*, 14916–14922.
(84) Langenbacher, T.; Immeln, D.; Dick, B.; Kottke, T. *J. Am. Chem. Soc.* **2009**, *131*, 14274–14280.
(85) Zeugner, A.; Byrdin, M.; Bouly, J.-P.; Bakrim, N.; Giovani, B.; Brettel, K.; Ahmad, M. *J. Biol. Chem.* **2005**, *280*, 19437–19440.
(86) Berndt, A.; Kottke, T.; Breitkreuz, H.; Dvorsky, R.; Hennig, S.; Alexander, M.; Wolf, E. *J. Biol. Chem.* **2007**, *282*, 13011–13021.
(87) Öztürk, N.; Song, S.; Selby, C.; Sancar, A. *J. Biol. Chem.* **2008**, *283*, 3256–3263.
(88) Phillips, J. B.; Jorge, P. E.; Muheim, R. *J. R. Soc. Interface* **2010**, *7*, S241–S256.
(89) Liu, B.; Liu, H.; Zhong, D.; Lin, C. *Curr. Opin. Plant Biol.* **2010**, *13*, 578–586.
(90) Brazard, J.; Usman, A.; Lacombat, F.; Ley, C.; Martin, M. M.; Plaza, P.; Mony, L.; Heijde, M.; Zabulon, G.; Bowler, C. *J. Am. Chem. Soc.* **2010**, *132*, 4935–4945.
(91) Chaves, I.; Pokorny, R.; Byrdin, M.; Hoang, N.; Ritz, T.; Rettel, K.; Essen, L.-O.; van der Horst, G. T.; Batschauer, L.; Ahmad, M. *Annu. Rev. Plant Biol.* **2011**, *62*, 335–364.
(92) O'Day, K. E. *PLoS Biol.* **2008**, *6*, 1359–1360.
(93) Kottke, T.; Batschauer, A.; Ahmad, M.; Heberle, J. *Biochem.* **2006**, *45*, 2472–2479.
(94) Schulten, K. *J. Chem. Phys.* **1985**, *82*, 1312–1316.
(95) Byrdin, M.; Sartor, V.; Eker, A. P.; Vos, M. H.; Aubert, C.; Brettel, K.; Mathis, P. *Biochim. Biophys. Acta* **2004**, *1655*, 64–70.
(96) Hogben, H. J.; Efimova, O.; Wagner-Rundell, N.; Timmel, C. R.; Hore, P. *Chem. Phys. Lett.* **2009**, *490*, 118–122.
(97) Schmidt, W. *Optical Spectroscopy in Chemistry and Life Sciences, an Introduction*; Wiley-VCH: New York, 2005.
(98) Gegear, R. J.; Casselman, A.; Waddell, S.; Reppert, S. M. *Nature* **2008**, *454*, 1014–1018.
(99) Foley, L. E.; Gegear, R. J.; Reppert, S. M. *Nature* **2011**.
(100) Efimova, O.; Hore, P. *Biophys. J.* **2008**, *94*, 1565–1574.
(101) Semm, P.; Beason, R. *Brain Res. Bull.* **1990**, *25*, 735–740.
(102) Alerstam, T. *J. Exp. Biol.* **1987**, *130*, 63–86.
(103) Lednor, A.; Walcott, C. *Behav. Ecol. Sociobiol.* **1988**, *130*, 3–8.
(104) Munro, U.; Munro, J.; Phillips, J. *Naturwissenschaften* **1997**, *84*, 26–28.
(105) Heyers, D.; Zapka, M.; Hoffmeister, M.; Wild, J.; Mouritsen, H. *Proc. Natl. Acad. Sci. U.S.A.* **2010**, *107*, 9394–9399.
(106) Kishkinev, D.; Chernetsov, N.; Mouritsen, H. *Auk* **2010**, *127*, 773–780.
(107) Wiltschko, W.; Wiltschko, R. *J. Comp. Physiol., A* **1999**, *184*, 295–299.
(108) Wiltschko, W.; Wiltschko, R.; Munro, U. *Naturwissenschaften* **2000**, *87*, 366–369.
(109) Wiltschko, W.; Munro, U.; Ford, H.; Wiltschko, R. *Proc. R. Soc. Lond. B* **2003**, *270*, 2133–2140.